Supplementary Information

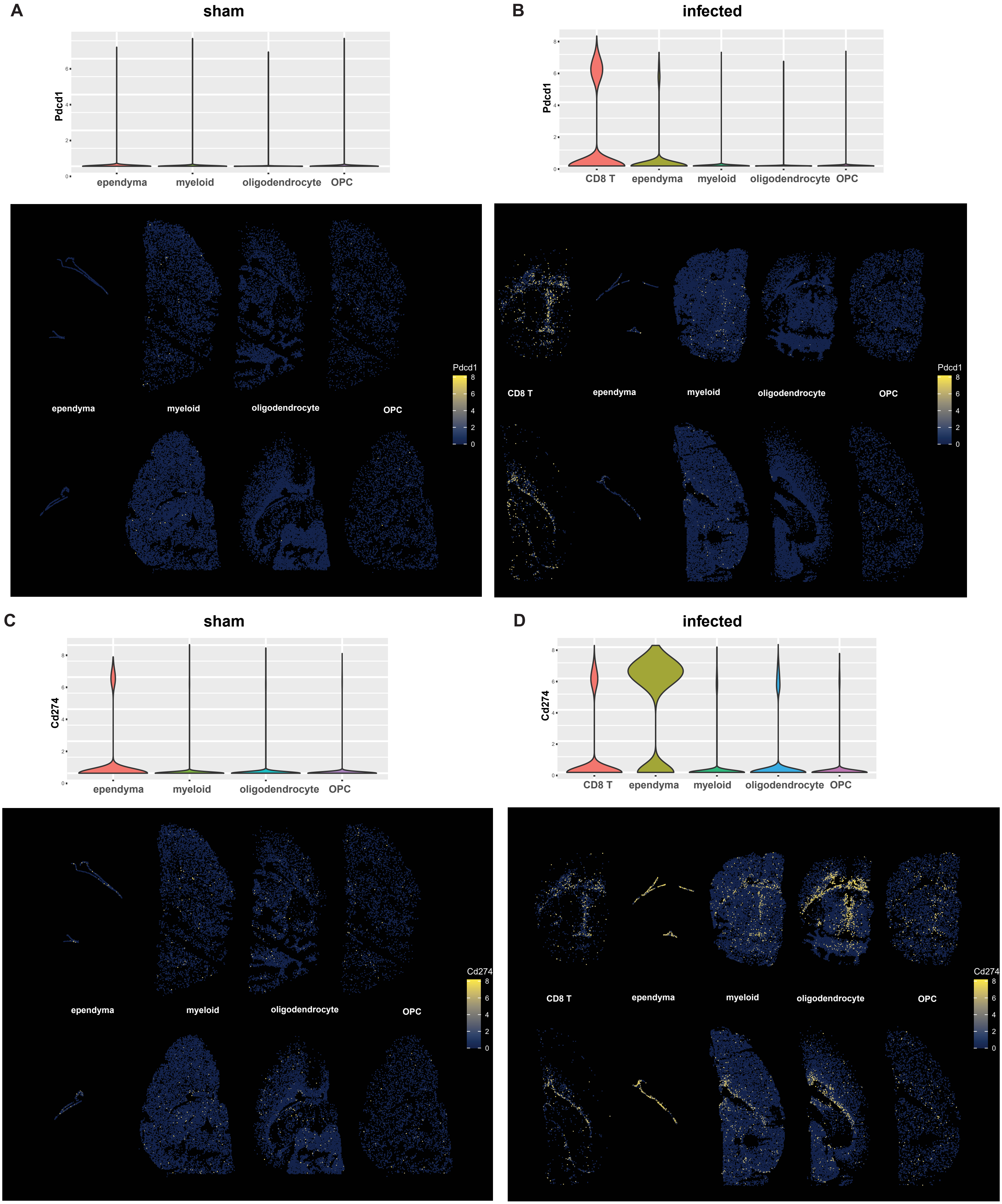

Supplementary Figure 1. MERFISH reveals spatial expression of Pdcd1 and Cd274 in the MuPyV-infected brain. WT mice were sham-injected with vehicle or infected with MuPyV i.c. Brains were collected at 8 dpi. **A)** Violin plot of *Pdcd1* expression in multiple cell types, along with two representative brain sections, in sham-injected mice. Spots indicate 8 x 8 µm spots, as determined by an image-based segmentation method[15], and are positioned according to their corresponding x and y coordinates, regardless of z coordinates. Spots are colored according to log-normalized *Pdcd1* transcript expression. **B)** shows *Pdcd1* expression similarly to A) in MuPyV-infected mice. **C)** shows *Cd274* expression in sham-injected mice, while **D)** shows *Cd274* expression in MuPyV-infected mice. n = 2 mice per condition. Numbers on y axes of violin plots refer to log-normalized expression of corresponding genes.

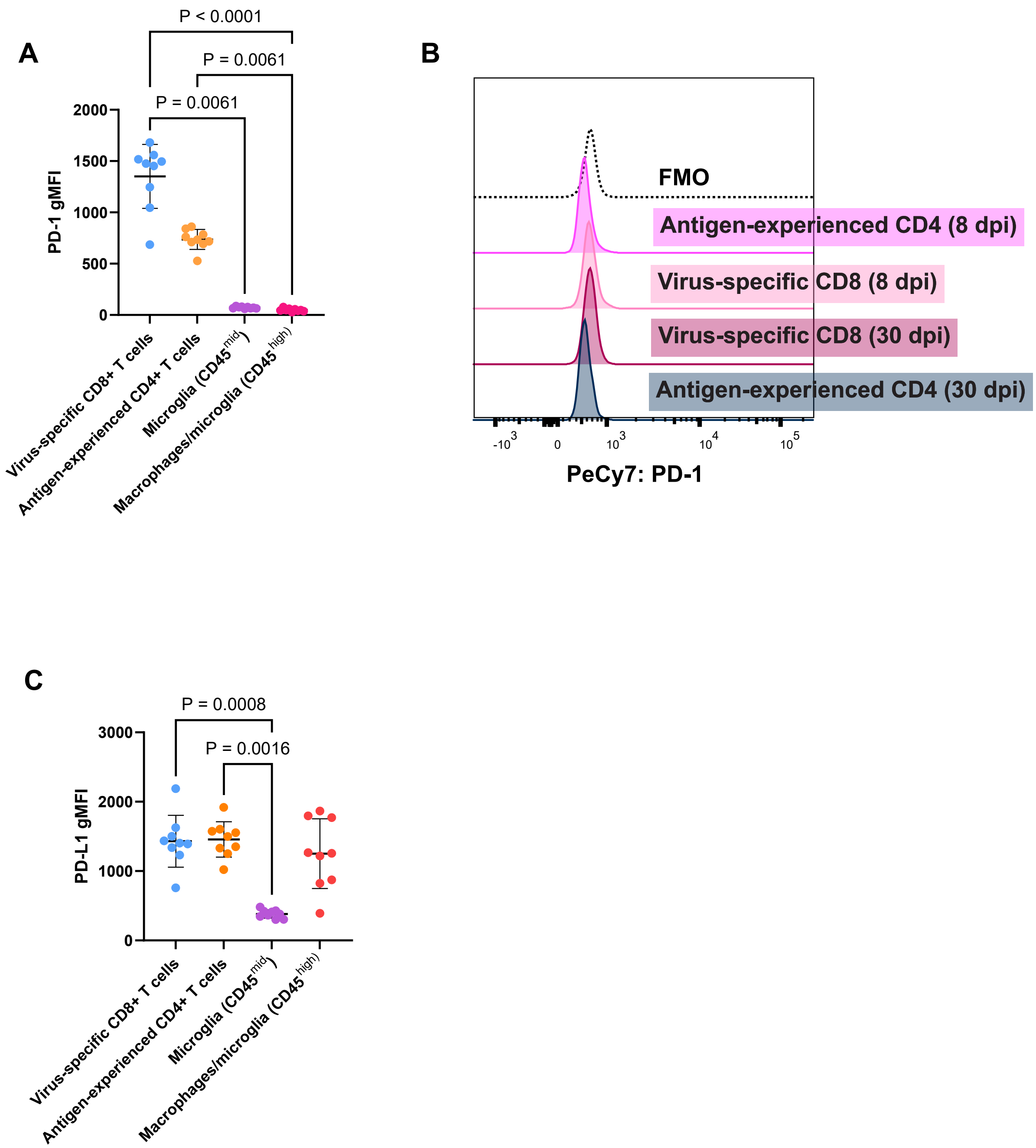

Supplementary Figure 2. PD-1 and PD-L1 expression are maintained on brain-infiltrating T cells during persistent infection. WT mice were infected with MuPyV i.c. At 8 and 30 dpi, cells were isolated from the brain and blood and analyzed for PD-1 and PD-L1 expression. Gating strategies are specified in Figure 1. **A)** PD-1 expression on different cell types in the brain at 30 dpi. **B)** Representative histogram of PD-1 expression on T cells in the blood at 8 and 30 dpi. **C)** PD-L1 expression on different cell types in the brain at 30 dpi. n = 8 mice for 8 dpi and 9 mice for 30 dpi. Error bars indicate mean ± SD. Data are representative of two independent experiments. As each mouse yielded all the immune cell types shown, statistical significance for A) and C) was calculated with the Friedman's test, a nonparametric alternative to the repeated measures one-way ANOVA, with a Dunn's post-test.

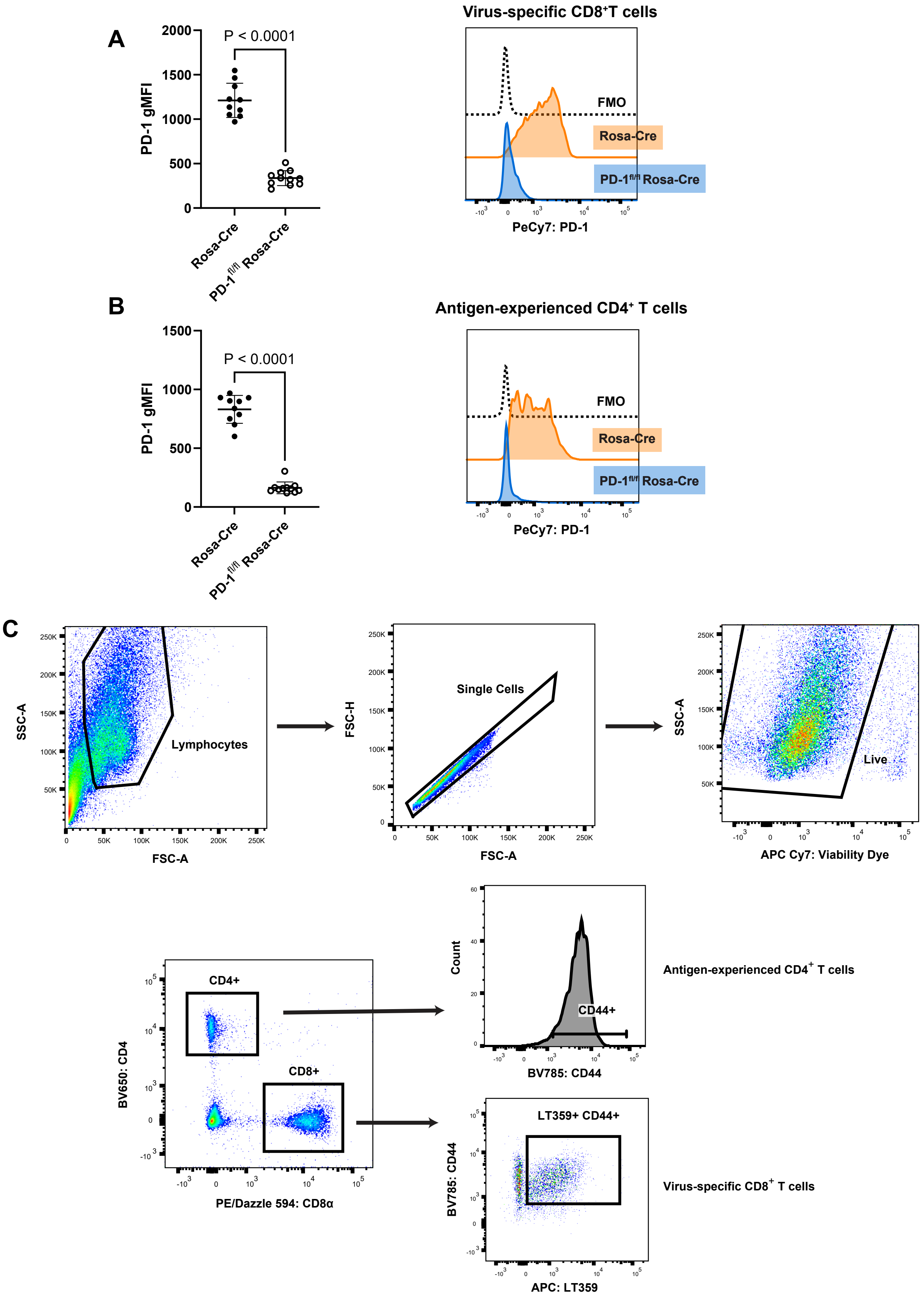

Supplementary Figure 3. Tamoxifen-induced knockdown of PD-1. Rosa-Cre controls and PD-1$^{fl/fl}$ Rosa-Cre mice were infected with MuPyV i.c., given tamoxifen 8 to 12 dpi, and brains dissected at 15 dpi. **A)** PD-1 expression on brain-infiltrating virus-specific CD8^{+} T cells. **B)** PD-1 expression on brain-infiltrating antigen-experienced CD4^{+} T cells. n = 10 Rosa-Cre mice and 11 PD-1$^{fl/fl}$ Rosa-Cre mice. Error bars are mean ± SD. Data show two combined independent experiments. Statistical significance was determined with a Mann-Whitney U test. C) Gating strategy for antigen-experienced (CD44^{+}) CD4^{+} and virus-specific (LT359^{+}) CD44^{+} CD8^{+} T cells, utilized for all flow cytometry experiments assessing these T cell populations in this study unless specified otherwise.

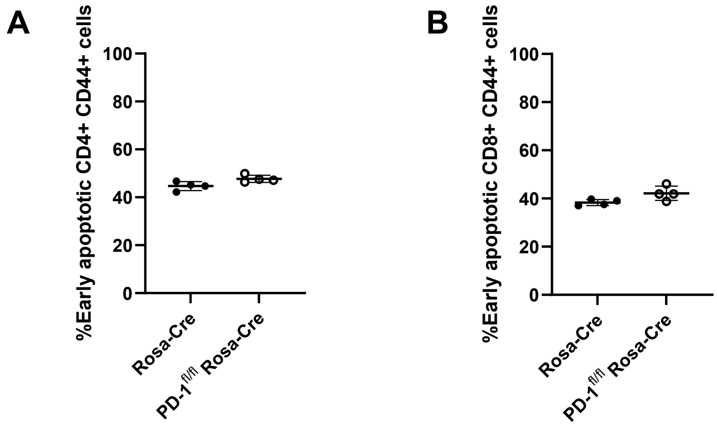

Supplementary Figure 4. Loss of PD-1 does not impact T cell apoptosis. Rosa-Cre mice and PD-1$^{fl/fl}$ Rosa-Cre mice were treated as in Supplementary 3. Cells were assessed for early apoptosis via positive staining for annexin V and negative expression of viability dye, which stains dead cells. **A)** Frequency of antigen-experienced CD4^{+} T cells undergoing early apoptosis. **B)** Frequency of virus-specific CD8^{+} T cells going through early apoptosis. n = 4 Rosa-Cre mice and 4 PD-1$^{fl/fl}$ Rosa-Cre mice. Statistical significance was calculated with a Mann-Whitney U test. Error bars indicate mean ± SD.

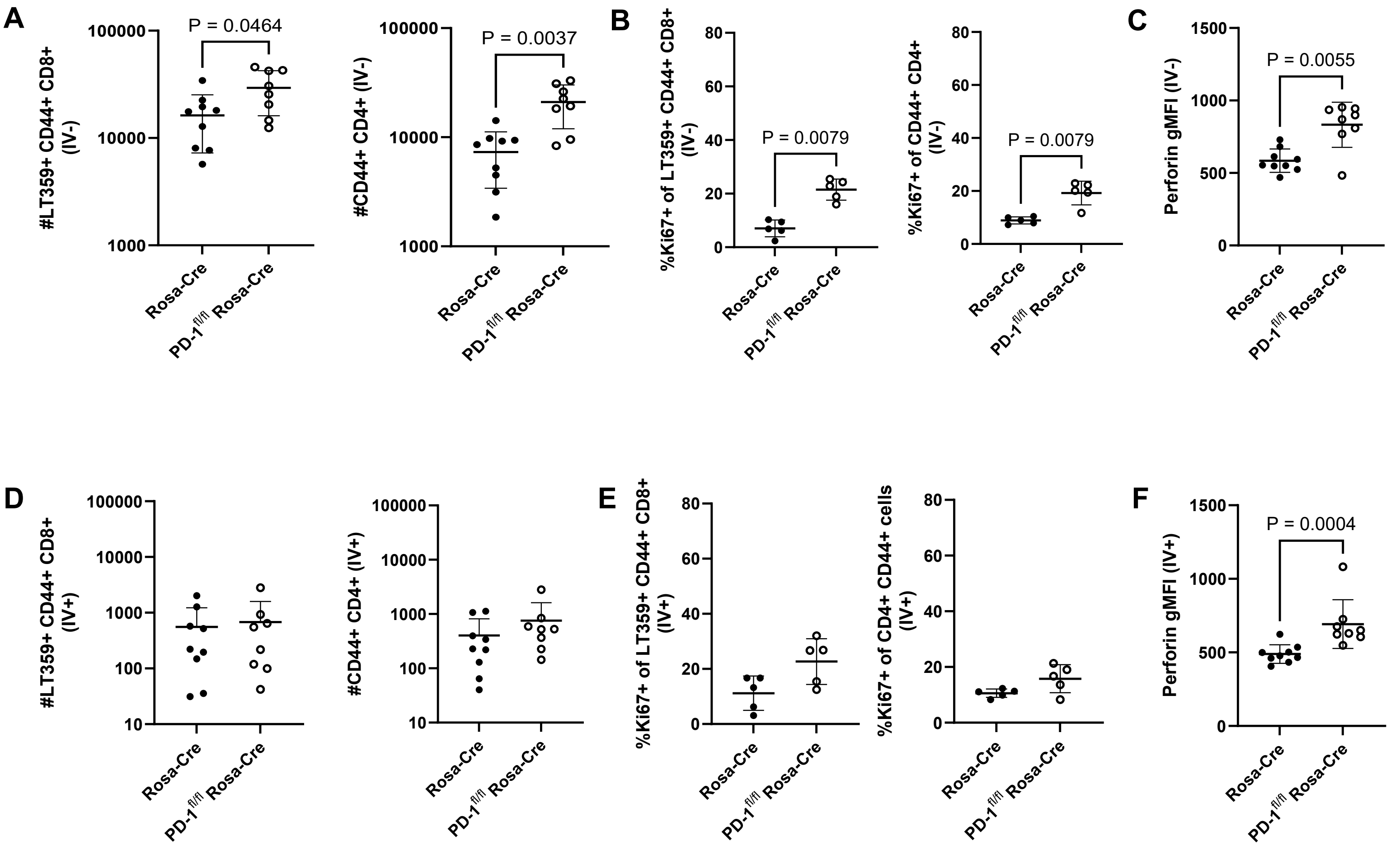

Supplementary Figure 5. Brain T cell phenotyping and quantification after CD45 antibody IV labeling. Rosa-Cre mice and PD-1$^{fl/fl}$ Rosa-Cre mice were treated as in Supplementary 3 and immediately prior to euthanasia were injected IV with fluorophore-conjugated anti-CD45. **A)** Numbers of brain-infiltrating (IV-) virus-specific CD8^{+} and antigen-experienced CD4^{+} T cells. **B)** Proportions of IV- T cells positive for proliferation marker Ki67. **C)** Perforin expression in IV- virus-specific CD8^{+} T cells. **D)** Numbers of T cells in the intravascular (IV+) compartment. **E)** Frequency of T cells expressing Ki67 in the IV+ compartment. **F)** Perforin expression in IV+ virus-specific CD8+ T cells. n = 9 Rosa-Cre mice and 8 PD-1$^{fl/fl}$ Rosa-Cre mice. Error bars are mean ± SD. Data combined from two independent experiments for all except B) and E), which are representative of two independent experiments. Statistical significance for all graphs was calculated with a Mann-Whitney U test.

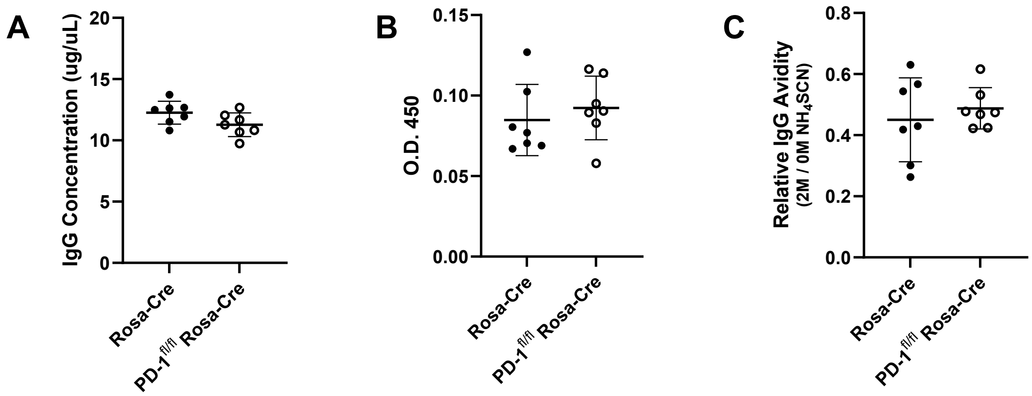

Supplementary Figure 6. PD-1 does not affect antiviral IgG or IgM. Sera were collected from Rosa-Cre and PD-1$^{fl/fl}$ Rosa-Cre treated as in Supplementary 3, and IgG and IgM were quantified by ELISA. **A)** Concentration of anti-MuPyV IgG. **B)** IgM levels, shown by absorption. **C)** Relative IgG avidity to MuPyV. n = 7 Rosa-Cre mice and 7 PD-1$^{fl/fl}$ Rosa-Cre mice. Data combined from two independent experiments. Statistical significance quantified with a Mann-Whitney U test. Error bars show mean ± SD.

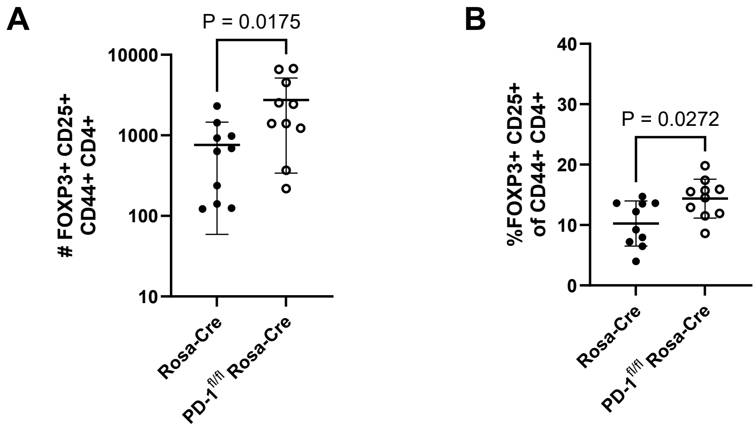

Supplementary Figure 7. PD-1 loss modestly increases T_{reg} cells in brains of MuPyV-infected mice. Mice were treated as in Supplementary 3. **A)** Numbers of T_{reg} cells, designated as $FOXP3^+$ $CD25^+$ $CD44^+$ $CD4^+$. **B)** Proportion of antigen-experienced $CD4^+$ T cells positive for FOXP3 and CD25. n = 10 Rosa-Cre mice and 10 PD-$1^{fl/fl}$ Rosa-Cre mice. Error bars show mean ± SD. Data combined from two independent experiments. Statistical significance calculated with a Mann-Whitney U test.

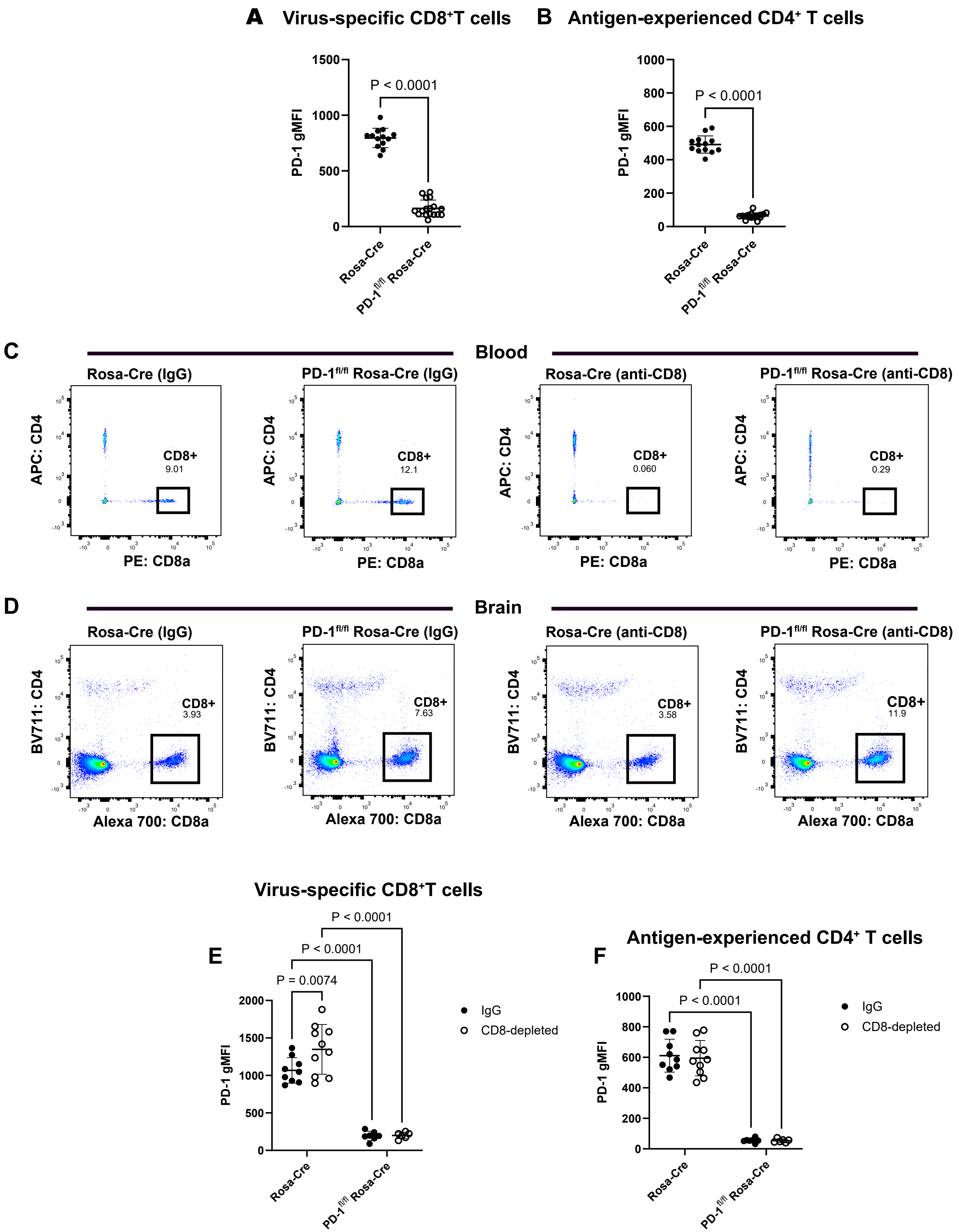

Supplementary Figure 8. T cells expand in a brain-autonomous manner after loss of PD-1 during persistent infection. A) PD-1 gMFI of virus-specific CD8$^+$ CD44$^+$ T cells and **B)** CD4$^+$ CD44$^+$ T cells in i.c. infected Rosa-Cre and PD-1$^{fl/fl}$ Rosa-Cre at 50 dpi (treated as in Fig. 3A). **C)** Representative flow cytometry plots showing CD8$^+$ and CD4$^+$ T cells in blood of IgG-treated and anti-CD8-treated mice (treated as in Fig. 3D). **D)** Representative flow cytometry plots showing CD8$^+$ and CD4$^+$ T cells in brains of IgG-treated and anti-CD8-treated mice. **E)** PD-1 gMFI of virus-specific CD8$^+$ CD44$^+$ T cells and **F)** CD4$^+$ CD44$^+$ T cells in i.c. infected IgG-treated and anti-CD8-treated Rosa-Cre and PD-1$^{fl/fl}$ Rosa-Cre at 50 dpi (treated as in Fig. 3D).

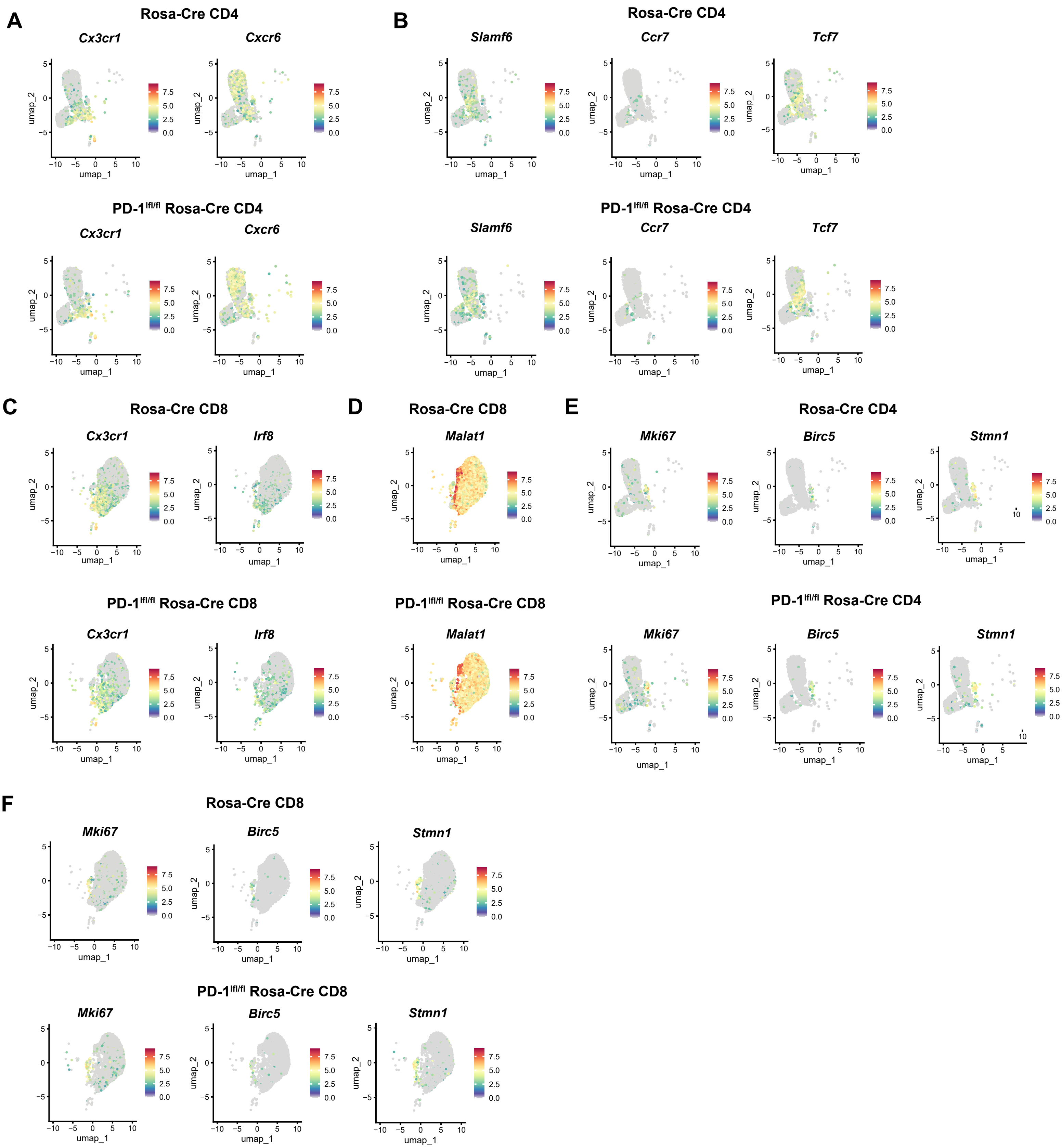

Supplementary Figure 9. Feature plots of genes in $CD4^+$ and $CD8^+$ T cell clusters. Virus-specific $CD8^+$ T cells and antigen-experienced $CD4^+$ T cells were sorted from pooled groups of Rosa-Cre and PD-1$^{fl/fl}$ Rosa-Cre mice, and processed for scRNA-seq. **A)** Feature plots for *Cx3cr1* and *Cxcr6* in antigen-experienced $CD4^+$ T cells. **B)** Feature plots for genes in cluster 6 of $CD4^+$ T cells. **C)** Genes in cluster 0 of virus-specific $CD8^+$ T cells. **D)** Feature plots for *Malat1* in cluster 8 of $CD8^+$ T cells. **E)** Feature plots of genes in cluster 7 in $CD4^+$ T cells. **F)** Feature plots of genes in cluster 7 in $CD8^+$ T cells. n = 10 mice per strain.

Rosa-Cre CD8 vs PD-1$^{fl/fl}$ Rosa-Cre CD8

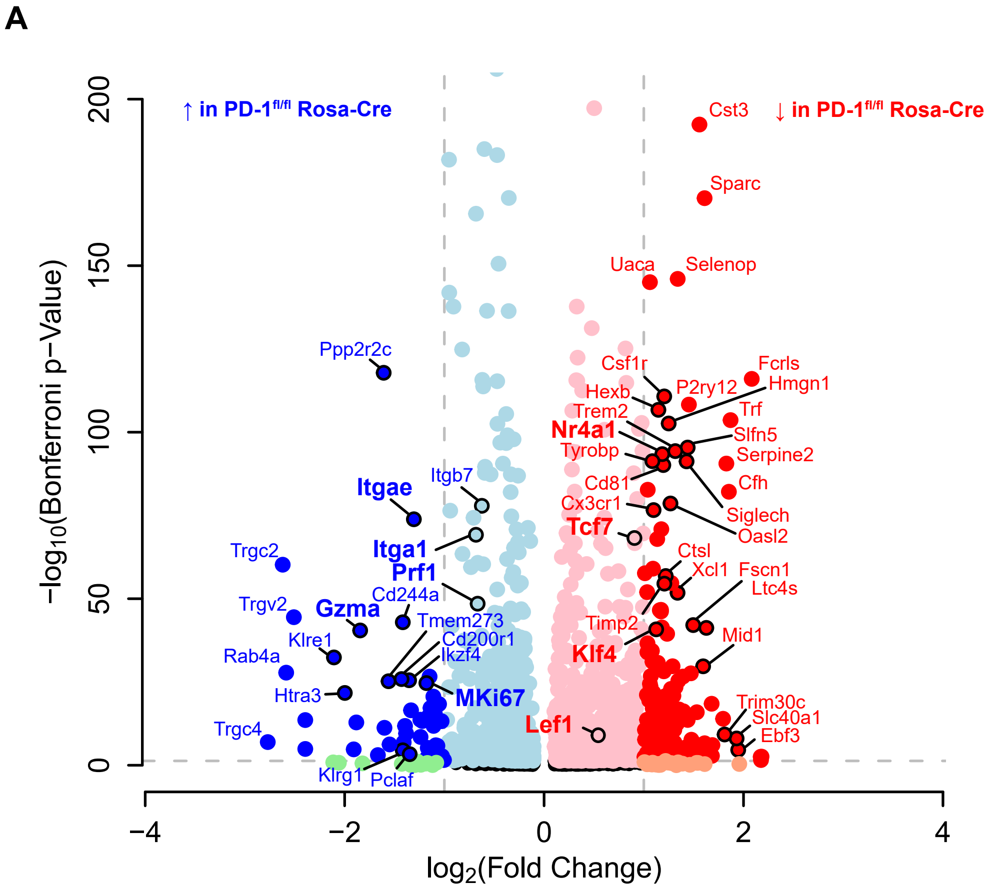

Rosa-Cre CD4 vs PD-1$^{fl/fl}$ Rosa-Cre CD4

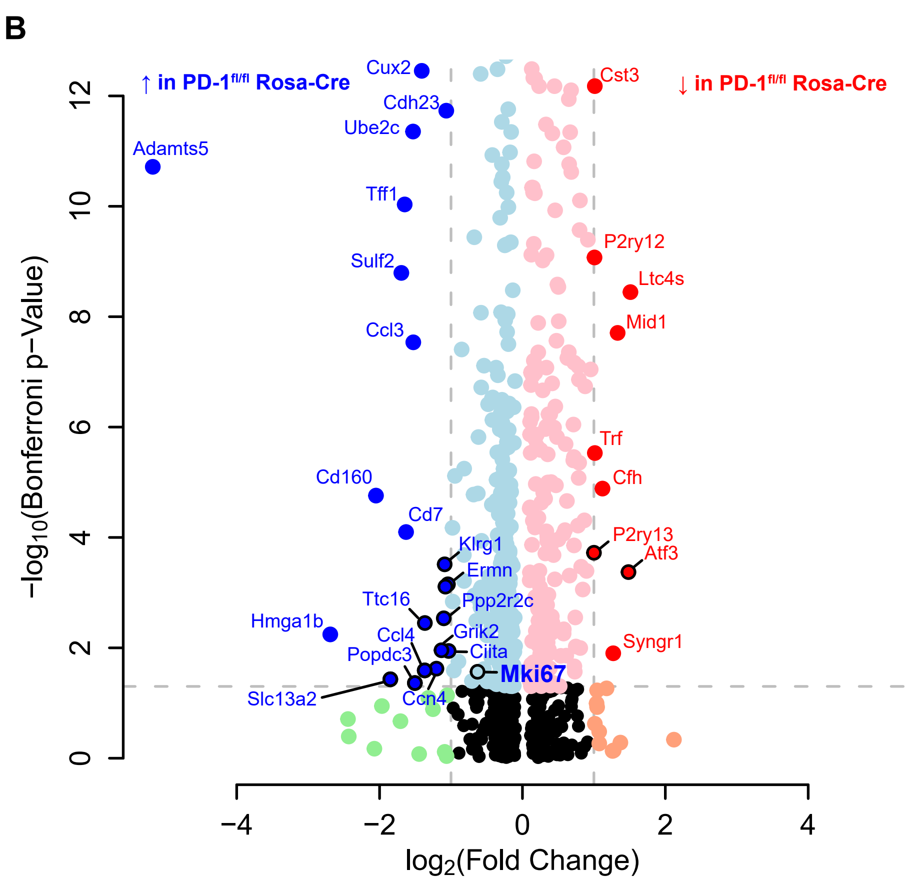

Supplementary Figure 10. Volcano plots showing differentially expressed genes in CD8$^+$ and CD4$^+$ T cells. Genes in blue are upregulated with loss of PD-1, and genes in red are downregulated with loss of PD-1. Bolded genes indicate ones associated with effector, resident memory-like, or proliferative phenotypes. **A)** Differentially expressed genes in CD8$^+$ T cells. **B)** Differentially expressed genes in CD4$^+$ T cells. n = 10 per mice. Thresholds set at log2 fold change below -1 and above 1 and above -log10(0.05).

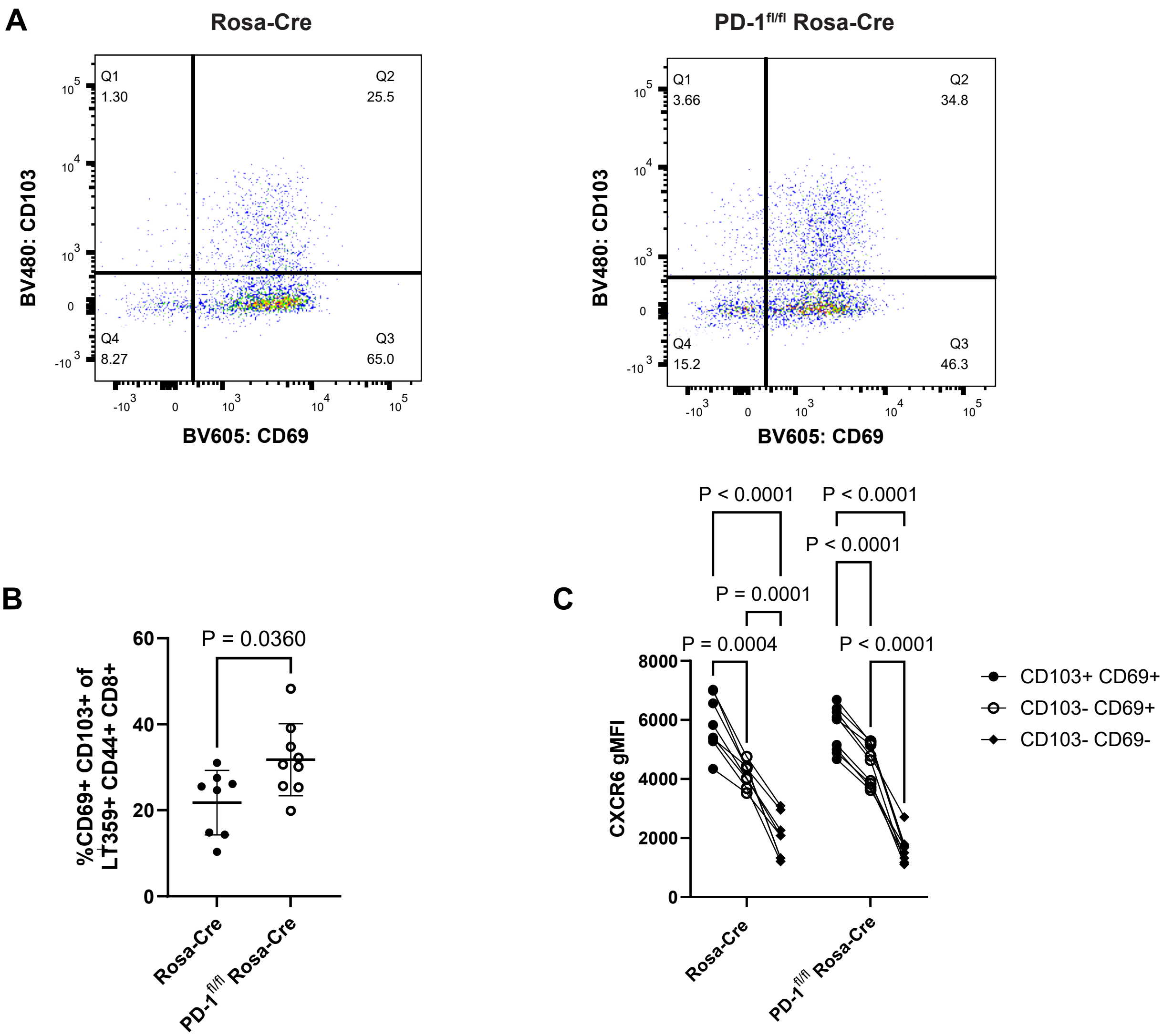

Supplementary Figure 11. Virus-specific CD103$^+$ CD8$^+$ T cells express CD69. PD-1$^{fl/fl}$ Rosa-Cre and Rosa-Cre mice were i.c. infected with MuPyV, and lymphocytes were isolated at 15 dpi. Mice were IV-labeled with CD45 antibody to identify circulating and brain-infiltrating cells. **A)** Representative flow cytometry plots from a Rosa-Cre mouse and a PD-1$^{fl/fl}$ Rosa-Cre mouse. Cells are gated from IV-negative (brain-infiltrating) virus-specific CD8$^+$ T cells and show co-expression of CD69 and CD103, both commonly used markers of tissue residency. **B)** Proportion of cells co-expressing CD103 and CD69 of virus-specific CD8$^+$ T cells. C) Virus-specific CD8$^+$ T cells were gated into three subsets, and CXCR6 gMFI compared across the three subsets. Error bars are mean ± SD. Statistical significance was calculated with a Mann-Whitney U test for A) and B). Two-way ANOVA, performed with matched values in mind, and Tukey's multiple comparisons post-test. Data combined from two independent experiments. n = 8 Rosa-Cre mice and 8 PD-1$^{fl/fl}$ Rosa-Cre mice.

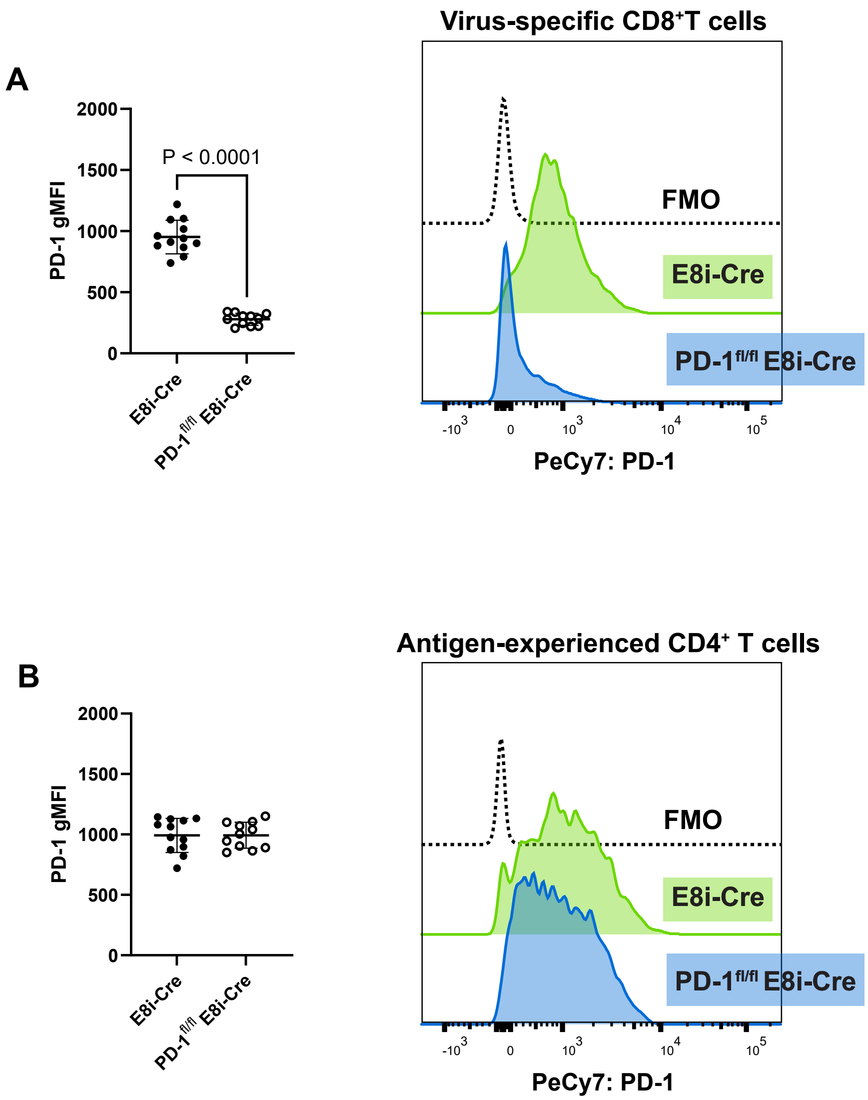

Supplementary Figure 12. CD8⁺ T cell-specific PD-1 knockdown. E8i-Cre controls and PD-1$^{fl/fl}$ E8i-Cre mice were i.c. inoculated with MuPyV, administered tamoxifen at 8 to 12 dpi, and T cells isolated from brains at 15 dpi. **A)** PD-1 expression on virus-specific CD8$^+$ T cells. **B)** PD-1 expression on antigen-experienced CD4$^+$ T cells. n = 12 E8i-Cre mice and 11 PD-1$^{fl/fl}$ E8i-Cre mice. Data combined from two independent experiments. Statistical significance calculated with a Mann-Whitney U test.

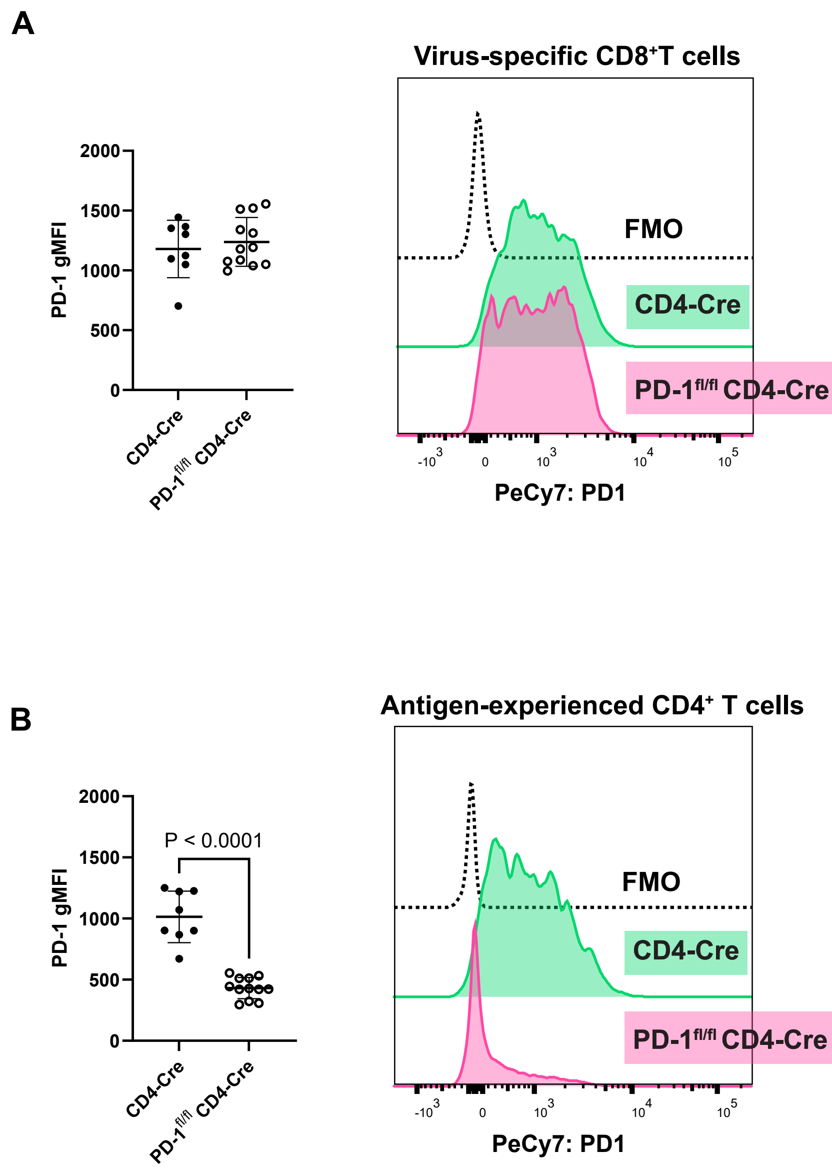

Supplementary Figure 13. CD4+ T cell-specific PD-1 knockdown. CD4-Cre mice and PD-1$^{fl/fl}$ CD4-Cre mice were infected with MuPyV i.c. and given tamoxifen at 8 to 12 dpi. Brains were phenotyped through flow cytometry at 15 dpi. **A)** PD-1 expression on virus-specific CD8^{+} T cells. **B)** PD-1 expression on antigen-experienced CD4^{+} T cells. n = 8 CD4-Cre mice and 12 PD-1$^{fl/fl}$ CD4-Cre mice. Data combined from two independent experiments. Statistical significance quantified with a Mann-Whitney U test.

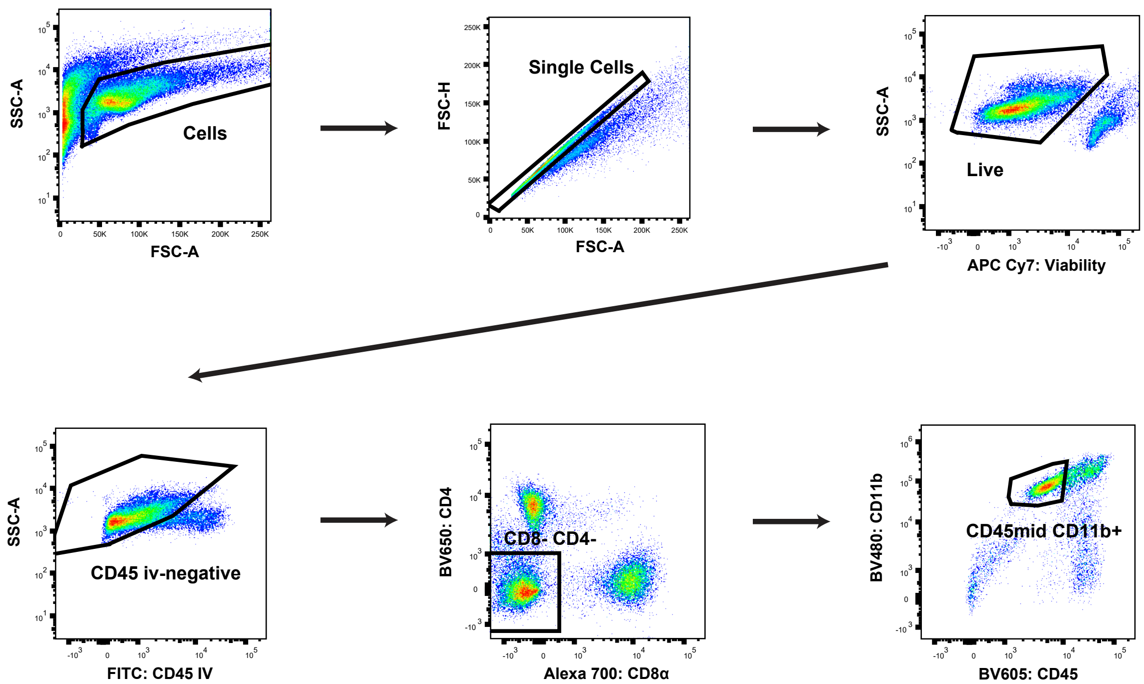

Supplementary Figure 14. Gating strategy for microglia. Representative gating strategy for CD45^{mid} CD11b^{+} microglia. Cells were IV-labeled with CD45 antibody, marking circulating cells.

Supplementary Table 1. List of Reagents or Resources used in Methods.

REAGENT or RESOURCE	SOURCE	IDENTIFIER	DILUTION (if applicable)
Antibodies			
Anti-annexin V PE	Biolegend	Cat. 640908	1:20
Anti-CD103 BV480 (Clone M290)	BD Biosciences	Cat. 566118	1:200
Anti-Cd11b BV480 (Clone M1/70)	BD Biosciences	Cat. 566149	1:200
Anti-CD19 FITC (Clone 1D3/CD19)	Biolegend	Cat. 152404	1:200
Anti-CD25 PerCPCy5.5 (Clone PC61)	Biolegend	Cat. 102029	1:200
Anti-CD3 PE (Clone 500A2)	Biolegend	Cat. 152310	1:100
Anti-CD4 APC (Clone RM4-5)	Biolegend	Cat. 100516	1:200
Anti-CD4 BV650 (Clone RM4-5)	Biolegend	Cat. 100546	1:200
Anti-CD4 BV711 (Clone RM4-5)	BD Biosciences	Cat. 563726	1:200
Anti-CD44 BV785 (Clone IM7)	Biolegend	Cat. 103059	1:200
Anti-CD45 AF700 (Clone 30.F11)	Biolegend	Cat. 103128	1:200
Anti-CD45 BV605 (Clone 30-F11)	Biolegend	Cat. 103155	1:200
Anti-CD45 FITC (Clone 30.F11)	Biolegend	Cat. 103108	1:200 3 mg per mouse for IV labeling
Anti-CD45 PerCPCy5.5 (Clone 30.F11)	Biolegend	Cat. 103132	1:200 3 ug per mouse for IV labeling
Anti-CD69 BV605 (Clone H1.2F3)	Biolegend	Cat. 104530	1:20
Anti-CD8α AF700 (Clone 53.6-7)	Biolegend	Cat. 100730	1:200
Anti-CD8α PE (Clone 53.6-7)	Biolegend	Cat. 100708	1:200
Anti-CD8α PE/Dazzle™ 594 (Clone 53.6-7)	Biolegend	Cat. 100762	1:200
Anti-CD8β (Clone H35-17.2)	Golstein et al., 1982	N/A	250 ug per mouse
Anti-CXCR6 BV711 (Clone SA051D1)	Biolegend	Cat. 151111	1:200
Anti-FOXP3 AF700 (Clone MF-14)	Biolegend	Cat. 126422	1:200
Anti-Granzyme B Pacific Blue™ (Clone GB11)	Biolegend	Cat. 515408	1:20
Anti-IFNγ APC (Clone XMG1.2)	BD Biosciences	Cat. 554413	1:200
Anti-IgM biotin	Biolegend	Cat. 406504	1:1000
Anti-IL-2 BV421 (Clone JES6-5H4)	Biolegend	Cat. 503826	1:200
Anti-MHCII (I-A/I-E) APC (Clone M5/114.15.2)	Biolegend	Cat. 107614	1:200
Anti-NK1.1 BV605 (Clone PK136)	Biolegend	Cat. 108739	1:200
Anti-PD-1 PeCy7 (Clone RMP1-30)	Biolegend	Cat. 109110	1:200

Anti-PDL1 BV421 (Clone MIH5)	BD Biosciences	Cat. 564716	1:200
Anti-Perforin PE (Clone S16009A)	Biolegend	Cat. 154306	1:200
Anti-TCF1 FITC (Clone 63D9)	Cell Signaling	Cat. 6444S	1:200
Anti-TNFα PE (Clone TN3-19.12)	Biolegend	Cat. 506104	1:200
ChromPure Rat IgG	Jackson Immunoresearch	Cat. 012-000-003	250 ug per mouse
eBioscience™ Anti-Ki67 AF700 (Clone SolA15)	Thermo Fisher Scientific Invitrogen™	Ref. 56-5698-82	1:200
Goat anti-IgG Heavy and Light Chain Antibody HRP Conjugated	Bethyl Laboratories	Cat. A90-116P	1:1000
HRP Goat Anti-IgG (minimal x-reactivity)	Biolegend	Cat. 405306	1:1000
LT359 APC	NIH Tetramer	Core/RRID:SCR_026557	1:200
Virus strains			
MuPyV, Strain A2	N/A	N/A	N/A
Chemicals, peptides, and recombinant proteins			
BD GolgiPlug™ Protein Transport Inhibitor (Containing Brefeldin A)	BD Biosciences	Cat. 51-2301KZ	1:200
Collagenase (Type I)	Worthington	Cat. LS004197	
Corn oil	Sigma-Aldrich	C8267	
DNAse I	Worthington	Cat. LS002140	
Percoll	Cytiva	Product 17089101	
Tamoxifen	Sigma-Aldrich	T5648	
Commercial assays			
1-Step™ TMB ELISA Substrate Solutions	Thermo Fisher Scientific	Ref. 34029	
BD Rhapsody WTA Reagent Kit - 8 Pack	BD Biosciences	Cat. 666620	
BD Rhapsody™ Cartridge Kit	BD Biosciences	Cat. 633733	
Bioanalyzer High Sensitivity DNA Analysis RUO	Agilent	Part No. 5067-4626	
eBioscience™ Foxp3 / Transcription Factor Staining Buffer Set	Thermo Fisher Scientific Invitrogen	Cat. 00-5523-00	
EIA/RIA Polystyrene High Bind Microplate	Corning	Ref. 3590	
MILLIPLEX® Mouse Cytokine Expansion Panel 1	Sigma Aldrich	MCYT1-190K-SPX	
Ms Single Cell Sample Multiplexing Kit	BD Biosciences	Cat. 633793	
PerfeCTa FastMix II ROX	QuantaBio	Part No. 95119-012	
Pierce BCA Protein Assay	Thermo Fisher	Cat. 23225	
Wizard Genomic DNA Purification Kit	Promega	Ref. A1120	
Experimental model organisms			
C57Bl/6J	Jackson Laboratories	Strain No. 000664	
CD4-CreERT2 C57BL/6J	Jackson Laboratories	Strain No. 022356	

E8i-Cre C57BL/6J	Andrews et al., 2021	N/A	
PD-1fl/fl C57BL/6J	Laurent Brossay at Brown University	N/A	
Rosa26 CreERT2	Jackson Laboratories	Strain No. 004847	
Software			
BCL Convert	Illumina	N/A	
Benchling	Benchling	RRID:SCR_013955	
Flowjo	BD Biosciences	RRID:SCR_008520	
Graphpad Prism	Dotmatics	RRID:SCR_002798	
ProcartaPlex	Thermo Fisher	N/A	
R v. 4.4.3	R Core Team 2021	RRID:SCR_001905	
Other			
BD Pharmingen™ Annexin V Binding Buffer, 10X concentrate	BD Biosciences	Cat. 556454	
BD Omics-Guard Sample Preservation Buffer	BD Biosciences	Cat. 570911	
eBioscience™ Fixable Viability Dye eFluor™ 780	Thermo Fisher Scientific Invitrogen™	Cat. 65-0865-14	1:1000
HRP Streptavidin	Biolegend	Cat. 405210	
MILLIPLEX MAP Lysis buffer for Multiplexing	Millipore Sigma	Cat. NC9471509	
Tissue-Tek® O.C.T. Compound	Sakura Finetek	Cat. 4583	
TRIzol™ Reagent	Thermo Fisher Scientific Invitrogen™	Cat. 15596018	